Journal of Rock Mechanics & Tunnelling Technology (JRMTT)
23 (1) 2017 pp 19-37

Available online at www.isrmtt.com

Effect of Transverse Isotropy of Rock Mass on Lined Pressure Tunnels using Finite Element Method

Siva Parvathi[*]*, T.V.Praveen*

Deptt. of Civil Engg., College of Engineering (A), Visakhapatnam, India

**Email: pagadala_sp@rediffmail.com*

ABSTRACT

Majority of tunnels for hydro-electric projects are located in mountainous region and the rock medium in which these excavations are made is usually non homogeneous and anisotropic. However, for most practical cases, anisotropic rocks are modeled as transversely isotropic media in a coordinate system attached to the directions of symmetry. In tunnel lining design, it is necessary to know the share of the rock load and internal pressure, on the lining. The share of the rock load or the support pressure on the lining depends on the quality of the rock mass. The stress analysis of lined pressure tunnels has been analyzed to study the effect of transverse isotropy of rock mass on lining for hard and intact rock (category-1). In the present study, the effect of Young's modulus (E/E') varies from 1 to 4, shear modulus (G/G') from 1 to 3 and Poisson's ratio (ν') from 0.1 to 0.5 have been considered to analyses for the transverse isotropic rock condition. The results are plotted for hoop stresses, shear stresses, radial stresses and radial displacement.

Keywords: Pressure tunnels; Transversely isotropy; Concrete lining; Stress analysis; Rock mass quality; Numerical modelling

1. INTRODUCTION

With increasing demand for water and urban mass transport, the design of tunnel system has become an important area of research. In pressure tunnels, the lining acts as a tunnel support system and it performs two important functions. Firstly, immediately after the excavation, it is needed to check the inward deformation of the excavation surface and to prevent any local collapse of loose rock blocks. Afterwards, it is needed to improve the aesthetics of the tunnel and to reduce the head loss as well as seepage in the case of power tunnels. The majority of tunnels for hydro-electric projects are located in rock formations and it is only in abnormal conditions that soft ground tunnelling enters into this field. The rock medium in which these excavations are constructed is non-homogeneous and anisotropic.

Structural design of tunnel lining requires a thorough study of the geology of the rock mass, the effective cover, results of in-situ tests for modulus of elasticity, Poisson's ratio, initial state of stress and other mechanical characteristics of rock. The lining should be designed such that the stresses in it are within the permissible limits in all types of loading conditions. In the design of concrete lining of the tunnel, it is necessary to consider the share of the rock load and internal pressure to be taken by the lining. Singh et al. (1995) have compared

support pressures measured from tunnels and caverns with estimates from Terzaghi's rock load concept. They found that the support pressure in rock tunnels and caverns does not increase directly with excavation size as assumed by Terzaghi (1946) and others, mainly because of dilatant behaviour of rock masses, joint roughness and prevention of loosening of rock mass by improved and modern tunnelling technology. They have subsequently recommended modified ranges of support pressures in both vertical (p_v) and horizontal (p_h) directions. Singh et al. (1997) have given approaches for the prediction of support pressure under squeezing and non-squeezing ground conditions. A study on effect of rock mass quality and tunnel size on lined pressure tunnels using FEM has been carried out by Siva Parvathi et al. (2005). Hoop stresses developed in the concrete lining for different rock mass conditions and tunnel sizes are presented. Study on influence of support pressure on stress variations in concrete lined pressure tunnels using FEM has been carried out by Siva Parvathi et al. (2015). The effect of support pressure on uncracked and cracked concrete lining conditions was studied. The effect of rock mass anisotropy on lining stresses has been studied by Kumar and Singh (1990). Elastic analysis of lined tunnel in isotropic medium is given by Jaeger (1972) and Kumar and Singh (1990) have extended the elastic theory to anisotropic rocks. For the analysis of pressure tunnel lining with simple physical and geological features of the rock mass, the finite element method is suitable.

Many rocks exposed near the earth's surface show well defined fabric elements in the form of bedding, stratification, layering, foliation, fissuring or jointing. In general, these rocks have properties (physical, dynamic, thermal, mechanical and hydraulic) that vary with direction and are said to be inherently anisotropic. Anisotropy can be found at different scales in a rock mass ranging from intact specimens to the entire rock mass.

Rock mass anisotropy can be found in volcanic formations (basalt, tuff) and sedimentary formation consisting of alternating layers or beds of different (isotropic or anisotropic) rock type. Rock mass cut by one or several regularly spaced joint sets are anisotropic in addition to being discontinuous. The rock between the joints can be isotropic or anisotropic. It is not unusual to have several types of planar anisotropy in a rock mass such as joints and foliation planes or joints and bedding planes. They are called foliation joints or bedding joints, respectively. The rocks mentioned above show clear evidence of anisotropy and were classified as class B anisotropy rocks by Barla (1974). On the other hand, Class A anisotropic rocks are those rocks that exhibit anisotropic properties despite apparent isotropy. Some intact granitic rocks belong to that group. The present work deals exclusively with rocks having intact and joint induced anisotropy.

The jointed rock mass has the special anisotropy that its shear modulus is very low compared to the modulus of elasticity, due to very low shear stiffness of rock joints at the low confining pressures.

2. DEFORMABILITY OF ANISOTROPIC ROCKS

2.1 Constitutive Modelling

The directional character of the deformability properties of anisotropic rocks and rock masses is usually assessed by field and laboratory testing. Deformability test results on anisotropic rocks are commonly analyzed in terms of the theory of elasticity for anisotropic media by assuming Hooke's law. The latter implies that the rock has at most 21 independent elastic components. However, for most practical cases, anisotropic rocks are often modelled as

orthotropic or transversely isotropic media in a coordinate system attached to their apparent structure or directions of symmetry. Orthotropic (orthorhombic symmetry) implies that three orthogonal planes of elastic symmetry exist at each point in the rock and that these planes have the same orientation throughout the rock. Transverse isotropy implies that at each point in the rock there is an axis of symmetry of rotation (n-fold axis of symmetry) and that the rock has isotropic properties in a plane normal to that axis. The plane is called the plane of transverse isotropy. For a rock mass that is orthotropic in a local n, s, t cartesian coordinate system (Fig. 1) attached to clearly defined planes of anisotropy, Hooke's law can be expressed as follows,

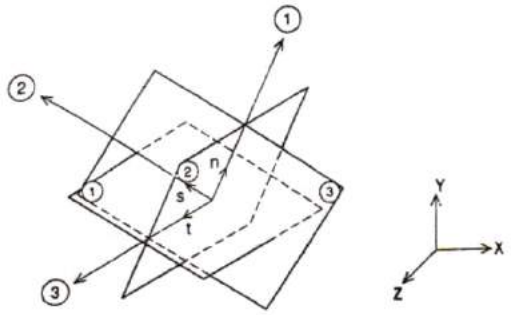

Fig.1: Orthotropic rock with three planes of symmetry normal to the n, s, t directions

$$\begin{bmatrix} \varepsilon_n \\ \varepsilon_s \\ \varepsilon_t \\ \gamma_{st} \\ \gamma_{nt} \\ \gamma_{ns} \end{bmatrix} = \begin{bmatrix} \frac{1}{E_n} & -\frac{\nu_{sti}}{E_s} & -\frac{\nu_{tri}}{E_t} & 0 & 0 & 0 \\ -\frac{\nu_{ns}}{E_n} & \frac{1}{E_s} & -\frac{\nu_{ts}}{E_t} & 0 & 0 & 0 \\ -\frac{\nu_{nt}}{E_n} & -\frac{\nu_{st}}{E_s} & \frac{1}{E_t} & 0 & 0 & 0 \\ 0 & 0 & 0 & \frac{1}{G_{st}} & 0 & 0 \\ 0 & 0 & 0 & 0 & \frac{1}{G_{nt}} & 0 \\ 0 & 0 & 0 & 0 & 0 & \frac{1}{G_{ns}} \end{bmatrix} \begin{bmatrix} \sigma_n \\ \sigma_s \\ \sigma_t \\ \tau_{st} \\ \tau_{nt} \\ \tau_{ns} \end{bmatrix} \quad (1)$$

or in more compact matrix form

$$(\varepsilon)_{nst} = (H)\,(\sigma)_{nst} \quad (2)$$

Nine independent elastic constants are needed to describe the deformability of the medium in n, s, t coordinate system. E_n, E_s, E_t are the Young's moduli in the n, s and t (or 1, 2 and 3) directions, respectively. G_{ns}, G_{nt} and G_{st} are the shear moduli in planes parallel to the ns, nt and st planes, respectively. Finally, ν_{ij} (i,j = n,s,t) are Poisson's ratios that characterize the normal strains in the symmetry directions j when a stress is applied in the symmetry directions i. because of symmetry of the compliance matrix (H), Poisson's ratios ν_{ij} and ν_{ji} are such that $\nu_{ij}/E_i = \nu_{ji}/E_j$.

Equations 1 and 2 still apply if the rock is transversely isotropic in one of the three ns, nt or st planes of Fig. 1. In that case, only five independent elastic constants are needed to describe the deformability of the rock in the n, s, t coordinate system. These constants are called E, E', ν, ν' and G' with the following definitions:

- E and E' are Young's moduli in the plane of transverse isotropy and in direction normal to it, respectively,
- ν and ν' are Poisson's ratios characterizing the lateral strain response in the plane of transverse isotropy to a stress acting parallel or normal to it, respectively and
- G' is the shear modulus in planes normal to the plane of transverse isotropy.

Relationships exist between E, E', ν, ν', G and G' and the coefficients of matrix (H) in Eqs. 1 and 2. For instance, for transverse isotropy in the st plane

$$\frac{1}{E_n} = \frac{1}{E'} ; \frac{1}{E_s} = \frac{1}{E_t} = \frac{1}{E} ; \frac{1}{G_{ns}} = \frac{1}{G_{nt}} = \frac{1}{G'}$$

$$\frac{\nu_{ns}}{E_n} = \frac{\nu_{nt}}{E_n} = \frac{\nu'}{E'} ; \frac{\nu_{st}}{E_s} = \frac{\nu_{ts}}{E_t} = \frac{\nu}{E} ; \frac{1}{G_{st}} = \frac{2(1+\nu)}{E} \quad (3)$$

The transverse isotropy formulation has been used to characterize the deformability of rocks such as schists, gneisses, phyllites, siltstones, mudstones, sandstones, shales and basalts. For such rocks, the plane of transverse isotropy is assumed to be parallel to foliation, schistosity or bedding planes. Some of the five or nine elastic constants of anisotropic rocks are sometimes assumed to be related. For instance, for transversely isotropic rocks, the modulus G' is often expressed in terms of E, E', ν and ν' through the following empirical equation.

$$\frac{1}{G'} = \frac{1}{E} + \frac{1}{E'} + 2\frac{\nu'}{E'} \quad (4)$$

The spatial orientation of the plane of transverse isotropy of rock mass for different orientations is as shown in the Fig. 2. The first case as shown in Fig. 2a deals the present study.

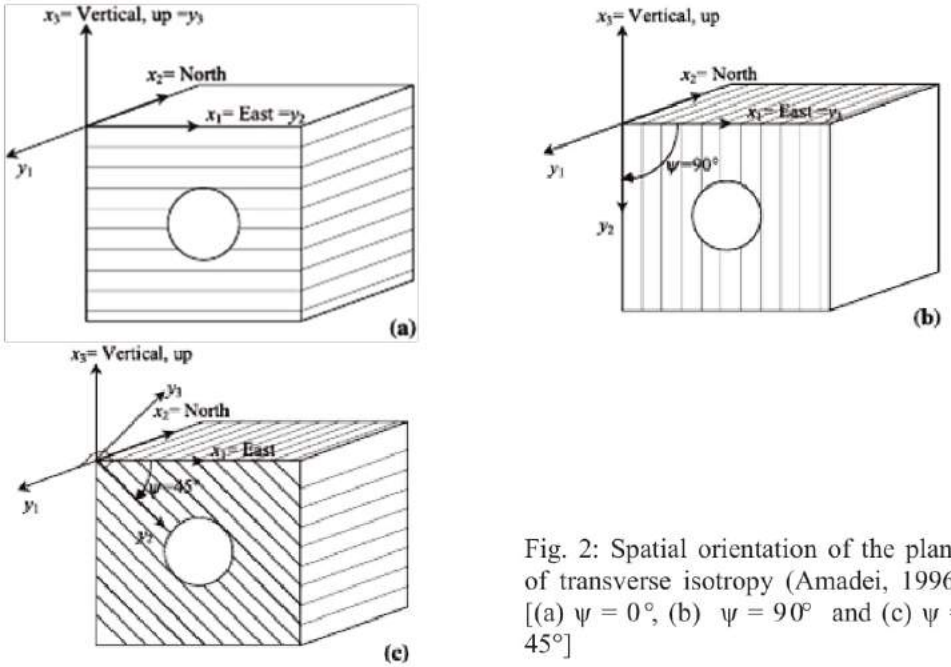

Fig. 2: Spatial orientation of the plane of transverse isotropy (Amadei, 1996) [(a) ψ = 0°, (b) ψ = 90° and (c) ψ = 45°]

A comprehensive review of literature indicates that finite element method is successfully used for analysis of pressure tunnels. Materials occurring in nature are seldom isotropic and homogenous. The general methods for solving problems involving non homogeneity and anisotropy are complex. It is possible to obtain sufficiently accurate results of displacement and stresses deep into the far-field without increasing the cost of analysis. So the present study intends to analyse the tunnel lining for transversely isotropic rock mass by using the finite element method.

Amadei et al. (1987) analyzed 98 measurements of elastic properties. They found that for most intact transversely isotropy rocks, the ratio E/E' varies between 1 and 4. Several cases of rocks with E/E' less than unity were found but did not fall 0.7. The ratio G/G' was found to vary between 1 and 3, the Poisson's ratio ν, between 0.1 and 0.35 and ν' between 0.1 and 0.7. The main objective of the present study is to analyze and study the effect of transverse isotropy of rock mass on lining stresses and lining-tunnel medium interaction for the following conditions: effect of Young's modulus (E/E'), effect of shear modulus (G/G') and effect of Poisson's ratio (ν').

3. MODELLING DETAILS

The lined pressure tunnels in transversely isotropic rock mass condition have been analysed using finite element method. The concrete lining and rock mass are modeled using 2-D plane strain isoparametric quadrilateral elements to represent long body and are suitable for structures subjected to plane loading. Concrete – rock interface is modeled with interface elements. The non-linearity introduced due to change in boundary at the interface, is modelled explicitly using 2-D gap and friction element is as shown in Fig. 3a. This boundary non-linearity arising at the interface due to the presence of two surfaces is represented using interface elements. In the boundary non-linearity, the material strain behaviour remains linear. The only nonlinear behaviour comes from changing of boundary at the interface i.e. contact between two or more bodies as in this case. In this approach the contact forces are updated incrementally until the system is balanced at the contact. This approach is numerically stable but requires more number of iterations and computation time to obtain the solution. Boundary non-linearity is considered in the present analysis.

This element is a 2-node interface element used to model node-to-node contact between two bodies. The element has two degrees of freedom, displacements in X and Y direction at each node consists of a pair of coupled orthogonal springs (Figs. 3b and 3c) in the normal and tangential directions. The element may assume open or closed status and may be sticking or sliding depending on whether the friction limit $\mu|f_n|$ is reached, where μ is the coefficient of friction and f_n is the normal compressive force in the gap. The load transfer between concrete and rock would depend upon the normal stiffness and tangential stiffness of the interface elements. The value of stiffness assumed is 1×10^9 N/m^2 as suggested by Kumar and Singh (1988). In the present work NISA (Numerically Integrated Elements for Systems Analysis) software package has been used to carry out the finite element analysis.

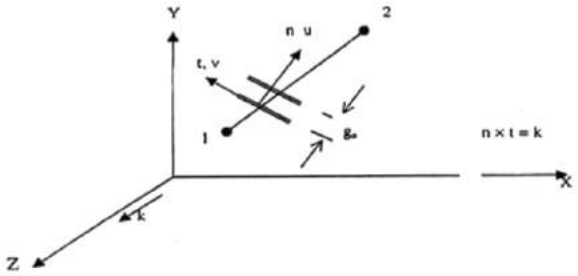

Fig. 3a: 2D Gap/friction element

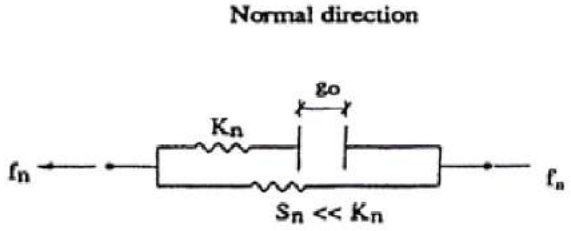

Fig. 3b: Stiff and soft springs in the normal direction

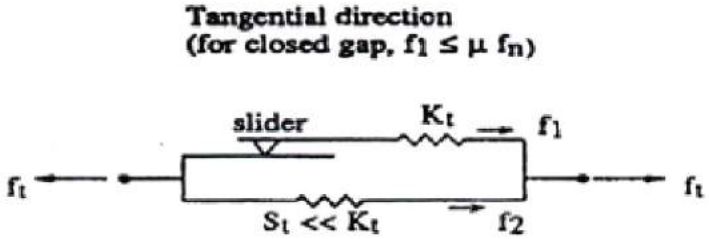

Fig. 3c: Stiff and soft springs in the tangential direction

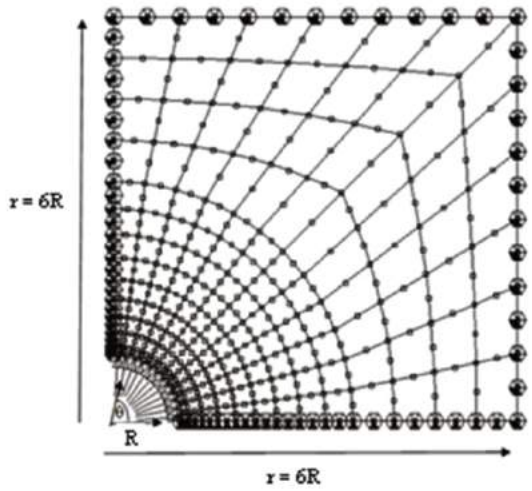

Fig. 4: Discretization of finite element model

3.1 Validation of the Modelling Procedure

For validation purpose, finite element analysis has been carried out for the concrete lined pressure tunnel subjected to internal water pressure. An opening of 5m radius and lined with concrete lining of thickness 0.1R (0.5m) is analyzed for internal water pressure of 1.0 $x10^5$ N/m^2. The finite element discretization of the problem is as shown in Fig. 4 and consists of 8-noded isoperimetric quadrilateral finite elements and 2 node interface elements of zero thickness. The boundary conditions of the domain are such that sides are roller supported and extreme boundaries are hinged. The rock-lining interface is simulated with the interface element (Siva Parvathi et al., 2013). The load transfer from rock to the concrete lining would depend upon the normal stiffness and the tangential stiffness of the interface elements. The value of stiffness placed is 1.0 $x10^9$ N/m^2. This problem is analysed in plane strain formulation for uniform internal water pressure. Since the problem is doubly symmetric, only one quadrant of the system is discretized. The horizontal axis corresponds to 0^0 while the vertical axis is placed at 90^0.The numerical values of various material constants are given in Table 1.

Table 1: Material properties for FE analyses

Material Properties	E_x, E_z (E) (N/m^2)	E_y (E') (N/m^2)	ν_{xz},(ν)	ν_{xy}, ν_{yz} (ν')	G_{xz} (G) (N/m^2)	G_{xy}, G_{yz} (G') (N/m^2)
Concrete	2.0 $x10^{10}$	2$x10^{10}$	0.15	-	8.6 x 10^8	-
Rock	2.0 $x10^9$	1 $x10^9$	0.2	0.375	8.3 x 10^8	3 x 10^8
	2.0 $x10^9$	1 $x10^9$	0.2	0.375	8.3 x 10^8	1.5 x 10^8
	2.0 $x10^9$	1 $x10^9$	0.2	0.375	8.3 x 10^8	0.5 x 10^8

Hence E_x, E_z and E_y are the modulus of elasticity in the horizontal and vertical directions, respectively; G is the shear modulus in horizontal direction; G' is the shear modulus in vertical direction; ν is the Poisson's ratio to account for effect of horizontal strain on complementary horizontal strain; ν' is the Poisson ratio to incorporate effect of vertical strain on horizontal strain. The stresses in the lining at some important locations i.e. at inner (R=b) and outer (R= c) surfaces of the concrete lining are given in Table 2. A good correlation between numerical and analytical values is observed.

Table 2: Lining stresses per unit water pressure

Location	Axis	Stress	Analytical value (Isotropic case)	Numerical value (Kumar and Singh, 1990)			Numerical value (Present study)		
				G =0.3E_V (N/m^2)	G=0.15 E_V (N/m^2)	G=0.05 E_V (N/m^2)	G =0.3E_V (N/m^2)	G=0.15 E_V (N/m^2)	G=0.05 E_V (N/m^2)
R = b	θ = 0°	σ_r	1.00	0.97	0.97	0.96	0.99	0.99	0.99
		σ_θ	-7.09	-7.28	-7.85	-8.40	-7.04	-7.53	-8.14
	θ = 90°	σ_r	1.00	0.95	0.94	0.94	1.00	1.00	1.00
		σ_θ	-7.09	-6.77	-7.34	-7.85	-6.50	-6.99	-7.57
R = c	θ = 0°	σ_r	0.23	0.19	0.14	0.08	0.29	0.22	0.16
		σ_θ	-6.32	-6.31	-6.81	-7.41	-5.97	-6.41	-6.82
	θ = 90°	σ_r	0.23	0.23	0.17	0.11	0.32	0.25	0.18
		σ_θ	-6.32	-6.32	-6.86	-7.5	-5.90	-6.45	-6.99

4. DETAILS OF THE PRESENT STUDY

The present study has been carried out on the feasibility of plain concrete tunnel lining. The tunnel is circular in cross section with an opening of 10 m diameter and concrete lining of 0.5m thicknesses. It is subjected to an internal water presser of $1.2x10^6$ N/m^2. The stress analysis has been carried out by the finite element method. For the analysis of the concrete lining with hard and intact rock mass case, as the external pressure is zero (Singh et al., 1995), only internal water pressure has been considered. The region of the domain and boundary conditions of the tunnel are as shown in Fig. 4. An opening of 5 m radius and lined with concrete lining of thickness 0.5 m is analyzed for internal water pressure. The displacement based finite element analysis is used. The FEM model consists of 8 noded isoparametric quadrilateral finite elements and 2 noded interface elements of zero thickness. The total number of elements is 181 and total number of nodes is 544 are considered in the discretization. This problem is analyzed in plane strain formulation under uniform water pressure. The numerical values of various material constants are given in Table 3. The properties of the lining remain unchanged while those of rock; vary in the sequence of Table 3. In the present study, the effect of Young's modulus (E/E') from 1 to 4, shear modulus (G/G') from 1 to 3 and Poisson's ratio (ν') from 0.1 to 0.5 have been considered for the study of transverse isotropic rock condition.

Table 3: Material constants for FE analysis

Material	E (N/m^2)	E' (N/m^2)	E/E'	ν	ν'	G × 10^5 (N/m^2)	G' ×10^5 (N/m^2)	G/G'
Concrete	2×10^{10}	----	----	0.15	-----	86956.92	-----	----
Rock Mass	$2x10^9$	$2x10^9$	1	0.2	0.2	8333.33	8333.33	1
	$2x10^9$	$1x10^9$	2	0.2	0.2	8333.33	8333.33	1
	$2x10^9$	$0.667x10^9$	3	0.2	0.2	8333.33	8333.33	1
	$2x10^9$	$0.5x10^9$	4	0.2	0.2	8333.33	8333.33	1
	$2x10^9$	$2x10^9$	1	0.2	0.2	8333.33	4166.66	2
	$2x10^9$	$1x10^9$	2	0.2	0.2	8333.33	4166.66	2
	$2x10^9$	$0.667x10^9$	3	0.2	0.2	8333.33	4166.66	2
	$2x10^9$	$0.5x10^9$	4	0.2	0.2	8333.33	4166.66	2
	$2x10^9$	$2x10^9$	1	0.2	0.2	8333.33	2777.77	3
	$2x10^9$	$1x10^9$	2	0.2	0.2	8333.33	2777.77	3
	$2x10^9$	$0.667x10^9$	3	0.2	0.2	8333.33	2777.77	3
	$2x10^9$	$0.5x10^9$	4	0.2	0.2	8333.33	2777.77	3
	$2x10^9$	$2x10^9$	1	0.2	0.1	8333.33	8333.33	1
	$2x10^9$	$2x10^9$	1	0.2	0.2	8333.33	8333.33	1
	$2x10^9$	$2x10^9$	1	0.2	0.3	8333.33	8333.33	1
	$2x10^9$	$2x10^9$	1	0.2	0.4	8333.33	8333.33	1
	$2x10^9$	$2x10^9$	1	0.2	0.5	8333.33	8333.33	1

5. RESULTS AND DISCUSSION

The results are plotted for hoop stress, shear stress, radial stress and radial displacement. Hoop stress variations are obtained from the stress analysis and are presented along two important radial lines, i.e., sidewall and crown which are subjected to maximum compressive

and tensile stresses around an opening. Hoop stresses are tensile and radial stresses are compressive and maximum stress concentrations are located in concrete lining for all the cases of lined tunnels. Shear stress distribution is plotted along concrete rock interface.

5.1 Effect of Young's Modulus on Lining

Figure 5 shows the hoop stress (σ_θ) variation along sidewall for different Young's modulus i.e. E/E' ratio varies from 1 to 4, G/G' and ν/ν' ratios equals to 1. From the Fig. 5, it is observed that maximum stresses are concentrated in the concrete lining only. The stresses in the concrete lining were completely tensile. In lined pressure tunnels, maximum hoop stresses are concentrated in the concrete lining, whereas in the rock mass, they suddenly decrease with the change in the material properties. As the E/E' ratio is increased, the maximum hoop stresses in the concrete lining are observed to increase. The inner surface of the concrete lining is subjected to the maximum tensile stress when compared to the outer surface of the concrete lining. As E/E' increases, the hoop stresses in the concrete lining increases in the plane of transverse isotropy of rock mass.

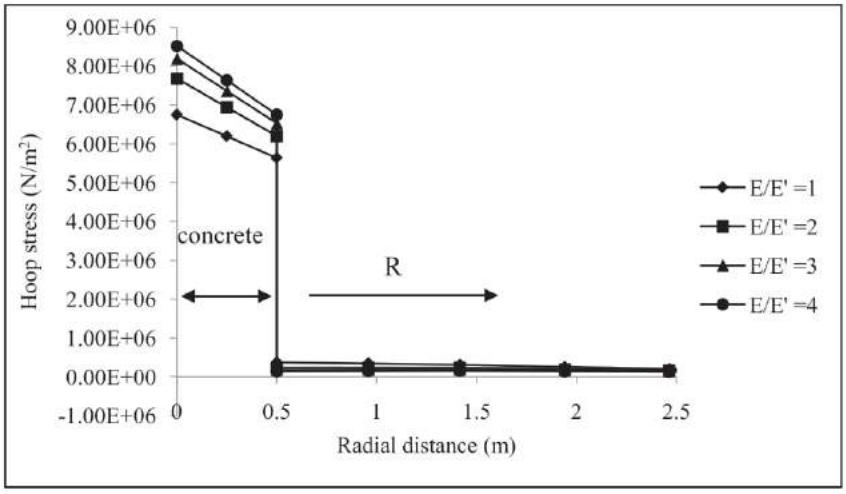

Fig. 5: Hoop stress variation along sidewall for different E/E' ratios

From Fig. 6, shows the hoop stress variation along crown for different Young's modulus i.e. E/E' ratio varies from 1 to 4, G/G' and ν/ν' ratios equals to 1. In this case also the maximum tensile stresses are observed to be in the concrete lining. As the E/E' ratio is increased the maximum hoop stresses are observed to be more uniform in the concrete lining. In the concrete lining, the hoop stresses in the direction normal to the plane of transverse isotropy is not much affected by the value of E/E' unlike the value of the hoop stress to the plane of transverse isotropy of rock mass. Maximum stresses are concentrated in the plane of transverse isotropy.

Shear stress variation along concrete rock interface has been plotted for different Young's modulus i.e. E/E' ratio and is as shown in Fig. 7. As the E/E' ratio is increased the shear stresses are observed to increase along the concrete rock interface. A non-uniform shear stress variation is observed along concrete rock interface.

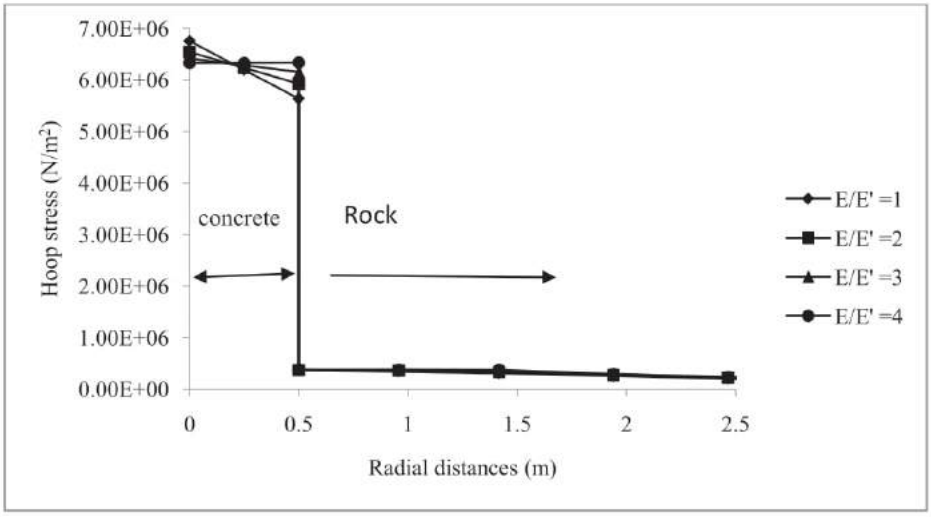

Fig. 6: Hoop stress variation along crown for different E/E' ratios

Figures 8 and 9 show the radial stress variation along sidewall and crown with radial distance for different Young's modulus i.e. E/E' ratio varies from 1 to 4, G/G' and ν/ν' ratios equals to 1. From the Fig. 8, it is observed that maximum stresses are concentrated in the inner surface of the concrete lining only. The stresses in the concrete lining were completely compression. As the E/E' ratio is increases, the maximum radial stresses in the concrete lining are observed to decrease. From the Fig. 9 it is observed that, in the concrete lining the value of the radial stress in a direction normal to the plane of transverse isotropy is not much affected by the value of E/E' unlike the value of the radial stress parallel to the plane of transverse isotropy of rock mass.

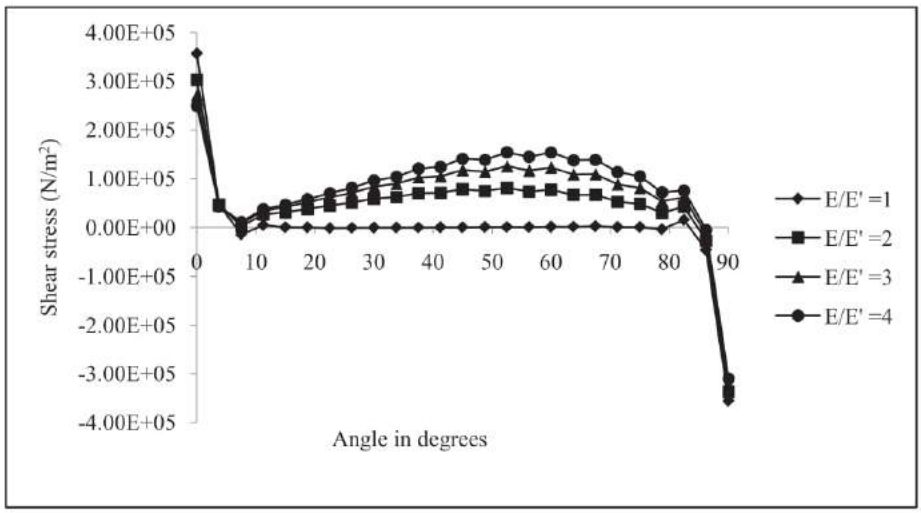

Fig. 7: Shear stress variation along the concrete rock interface for different E/E' ratios

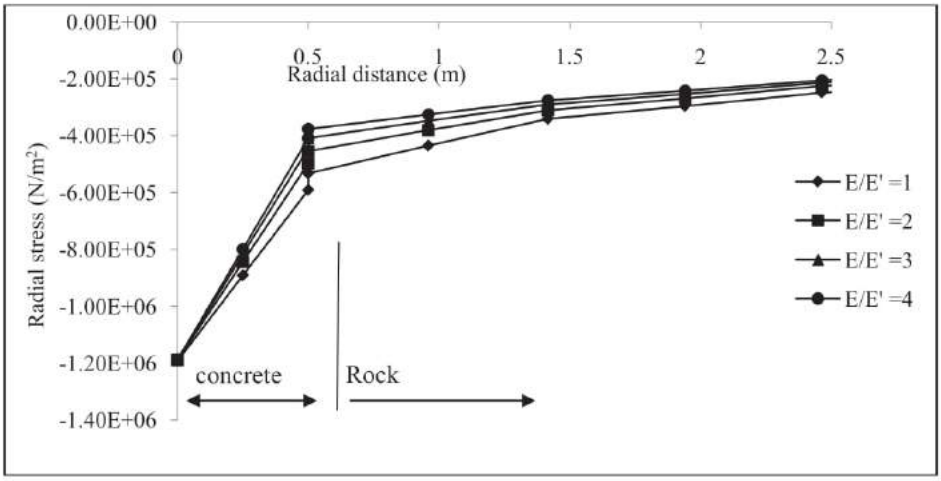

Fig. 8: Radial stress variations along side wall for different E/E' ratios

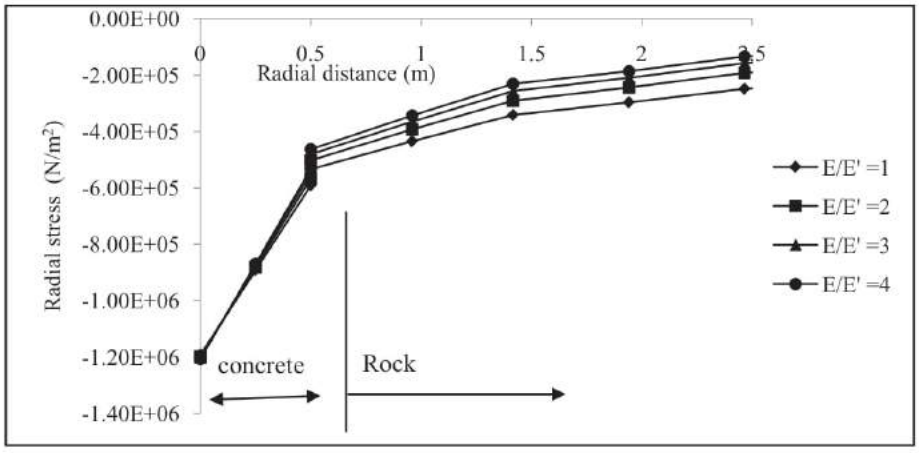

Fig. 9: Radial stress variations along crown for different E/E' ratios

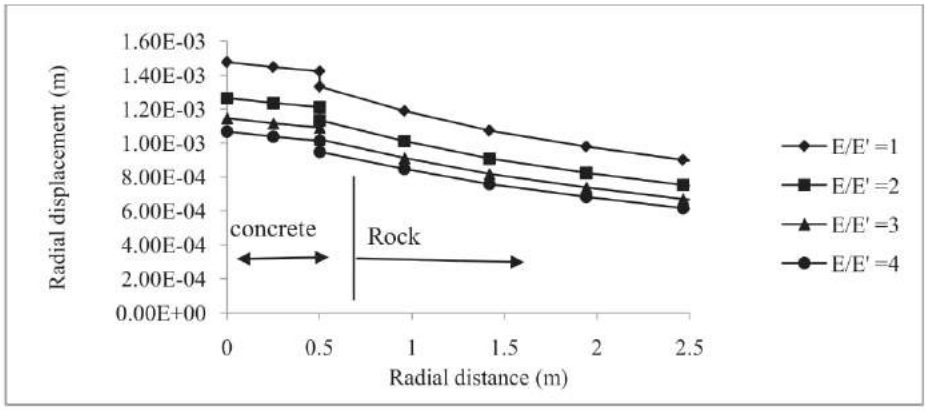

Fig. 10: Radial displacement variation along side wall for different E/E' ratios

Figures 10 and 11 show the radial displacement variation along sidewall and crown with radial distance for different Young's modulus i.e. E/E' ratio. From the Fig. 10, it is observed that maximum radial displacements are concentrated in the concrete lining only. As the E/E' ratio is increased, the maximum radial displacement in the concrete lining are observed to decrease along side wall. From the Fig. 11, it is observed that, as the E/E' ratio is increased, the maximum radial displacements in the concrete lining are observed to increase along crown.

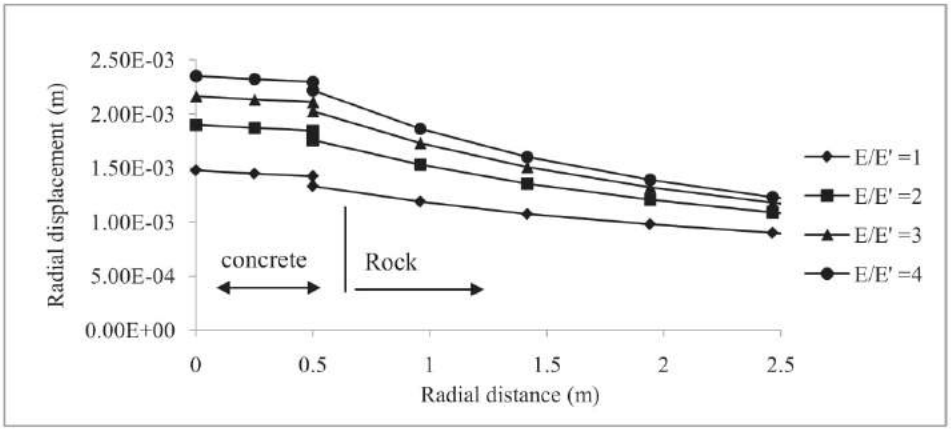

Fig. 11: Radial displacement variation along crown for different E/E' ratios

5.2 Effect of Shear Modulus on Lining

Figure 12 shows the hoop stress variation along sidewall with radial distance for different shear modulus i.e. G/G' ratio varies from 1 to 3, E/E' and ν/ν' ratios equals to 1. The stresses in the concrete lining were completely tensile. As the G/G' ratio is increased, the maximum hoop stresses in the concrete lining are observed to increase. The inner surface of the concrete lining is subjected to the maximum tensile stresses when compared to the outer surface of the concrete lining. As G/G' increases, the hoop stresses in the concrete lining increases in the direction of plane of transverse isotropy of rock mass.

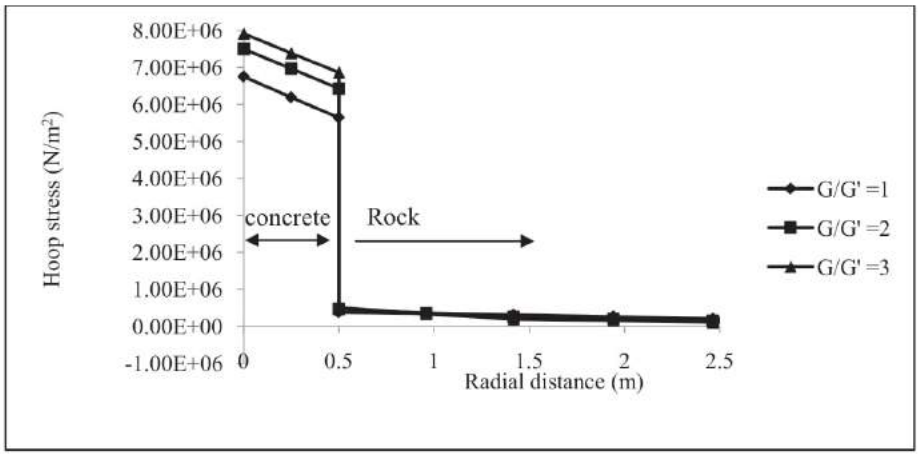

Fig.12: Hoop stress variation along sidewall for different G/G' ratios

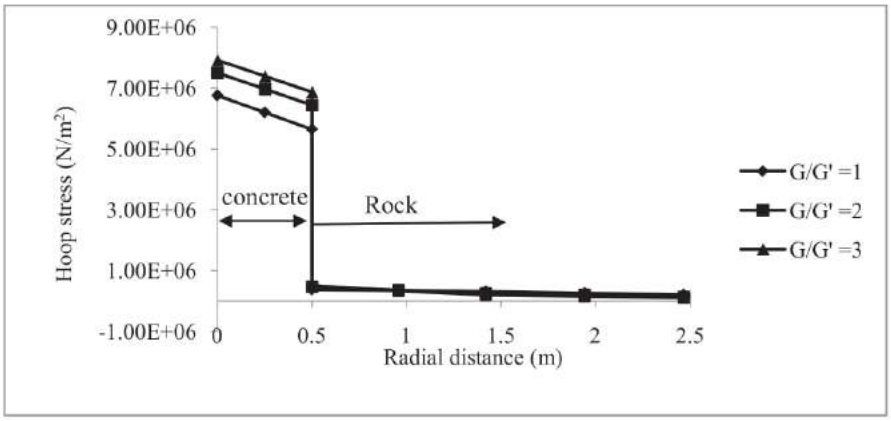

Fig.13: Hoop stress variation along crown for different G/G' ratios

Figure13 shows the hoop stress variation along crown for different shear modulus i.e. G/G' ratio. As G/G' increases, the hoop stresses in the concrete lining increases in both the directions parallel and normal to the plane of transverse isotropy of rock mass. Shear stress variation along concrete rock interface has been plotted for different shear modulus i.e. G/G' and is as shown in Fig. 14. From the Fig. 14 it has been observed that the effect of shear modulus (G/G') is not observed in shear stress distribution along concrete-rock interface.

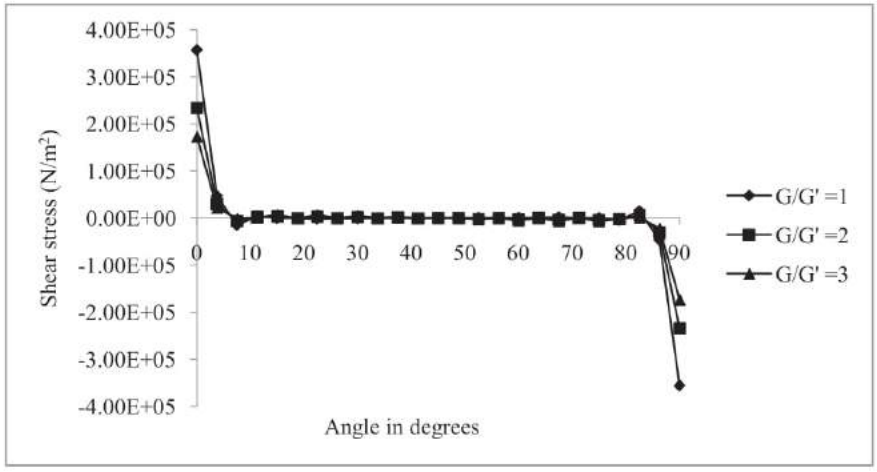

Fig.14: Shear stress variation along the concrete-rock interface for different G/G' ratios

Figures15 and 16 show the radial stress variation along sidewall and crown with radial distance for different shear modulus i.e. G/G' ratio. Similar radial stress variation is observed along side wall and crown. From the Figs. 15 and 16, it is observed that maximum stresses are concentrated in the concrete lining and are completely under compression. As the G/G' ratio is increased, the maximum radial stresses in the concrete lining are observed to be decreased.

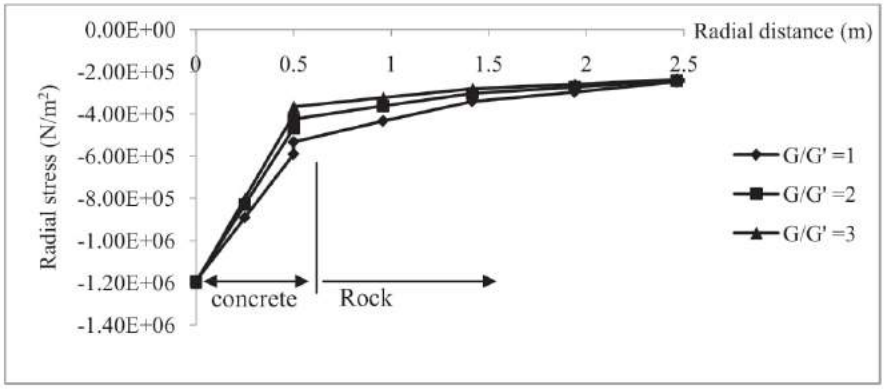

Fig. 15: Radial stress variations along side wall for different G/G' ratios

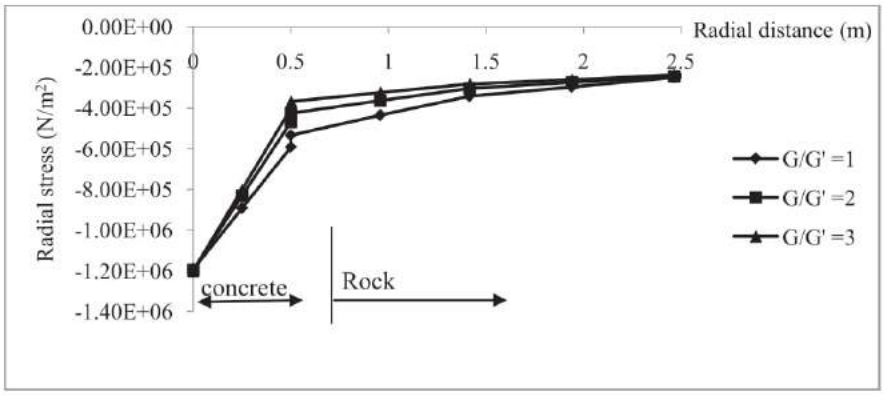

Fig. 16: Radial stress variations along crown for different G/G' ratios

Figs.17 and 18 shows the radial displacement variation along sidewall and crown with radial distance for different shear modulus. Similar variation is observed along side wall and crown. From the Figs. 17 and 18, it is observed that maximum radial displacements are concentrated in the concrete lining only. As the G/G' ratio is increases, the maximum radial displacements in the concrete lining are observed to be increase.

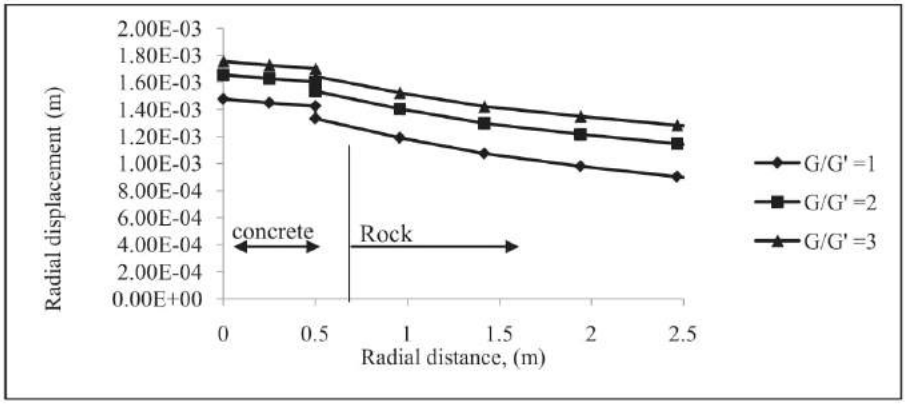

Fig. 17: Radial displacement variation along side wall for different G/G' ratios

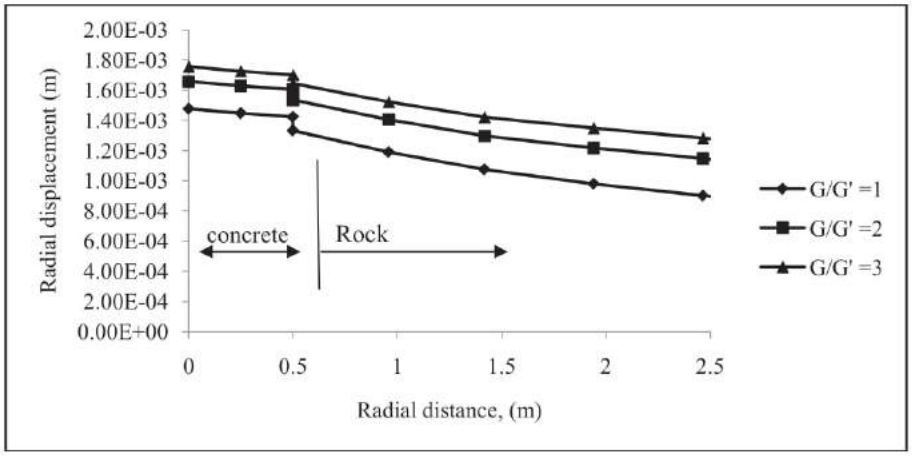

Fig. 18: Radial displacement variation along crown for different G/G' ratios

5.3 Effect of Poisson's Ratio on Lining

Fig.19 shows the hoop stress variation along sidewall with radial distance for different Poisson's ratio i.e. ν' values varies from 0.1 to 0.5, G/G' and E/E' ratios equals to 1. The stresses in the concrete lining were completely tensile. As the ν' value is increased, the hoop stress variation in the concrete lining is observed to be insignificant. The inner surface of the concrete lining is subjected to the maximum tensile stresses when compared to the outer surface of the concrete lining.

Figure 20 shows the hoop stress variation along crown for different Poisson's ratio. In this case also the maximum tensile stresses are observed to be in the inner surface of the concrete lining. As the ν' value is increased, a marginal increase in the hoop stress variations is observed in the concrete lining. Shear stress variation along concrete rock interface has been plotted for different Poisson's ratio and is as shown in Fig. 21. As the ν' value is increased, marginal increase in the shear stress is observed along the concrete rock interface. A non-uniform shear stress variation is observed along concrete rock interface.

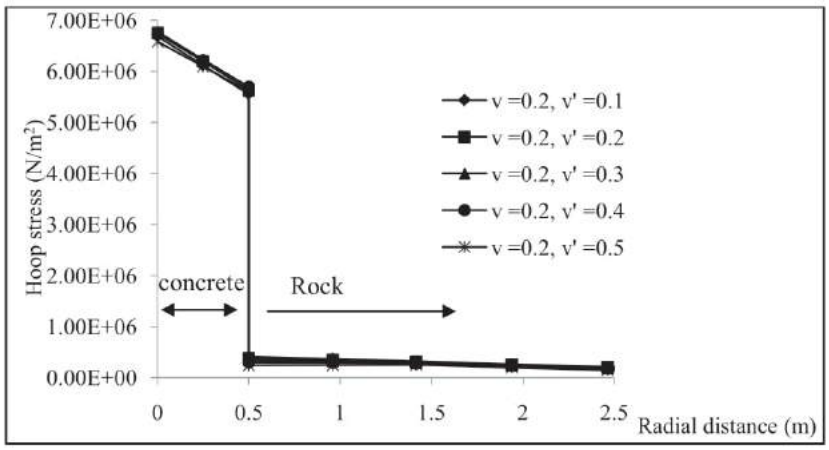

Fig. 19: Hoop stress variation along sidewall for different ν' values

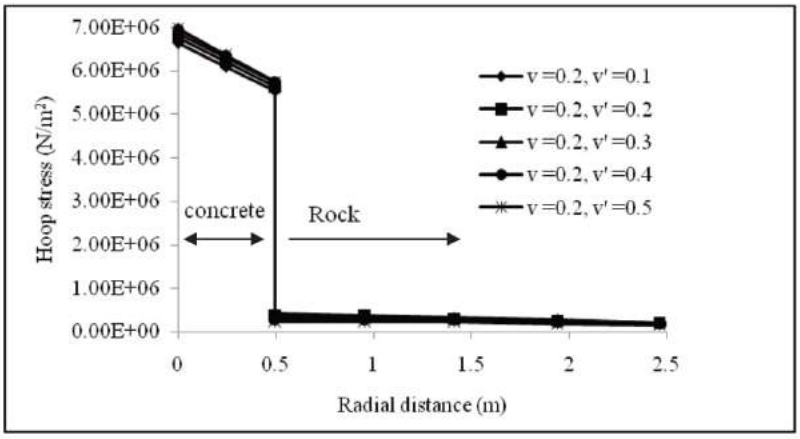

Fig. 20: Hoop stress variation along crown for different ν' values

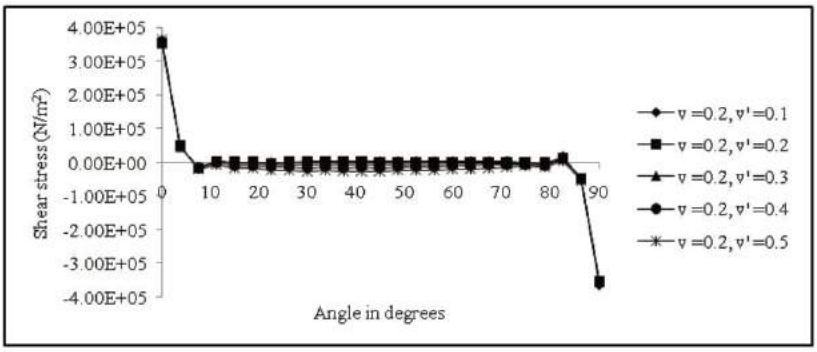

Fig. 21: Shear stress variation along the concrete-rock interface for different ν' values

The radial stress variation along side wall and crown for different ν' values varies from 0.1 to 0.5 and are as shown in the Figs. 22 and 23. Similar stress variation is observed along side wall and crown. From the Figs. 22 and 23, it is observed that maximum stresses are concentrated in the concrete lining are completely under compression. The effect of ν' is observed insignificant in radial stress variation.

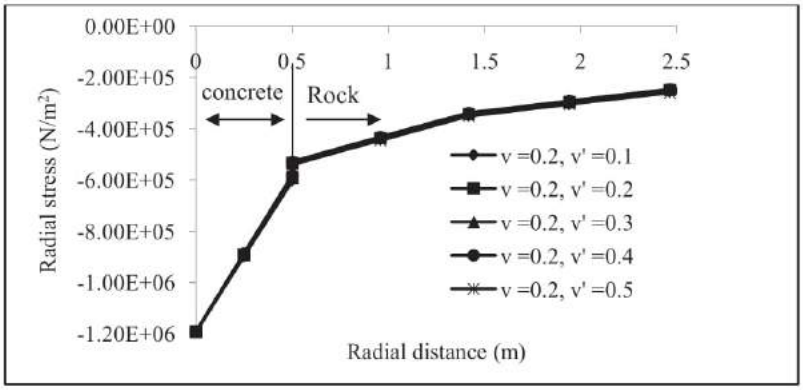

Fig. 22: Radial stress variations along side wall for different ν' values

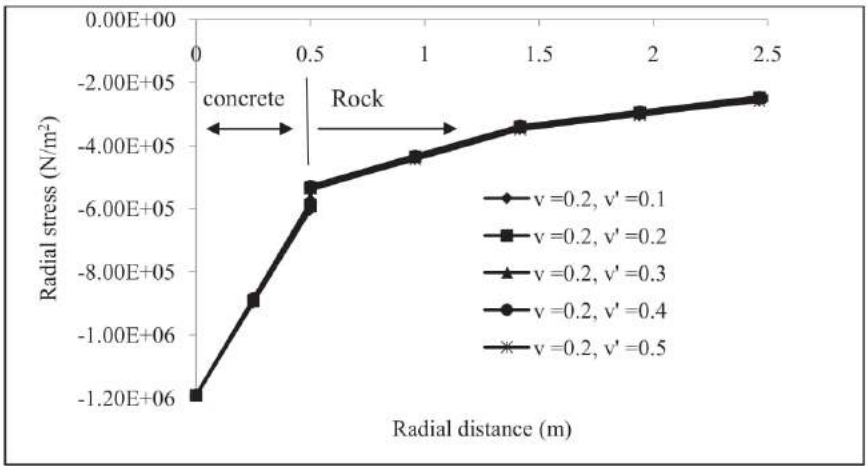

Fig. 23: Radial stress variations along crown for different ν' values

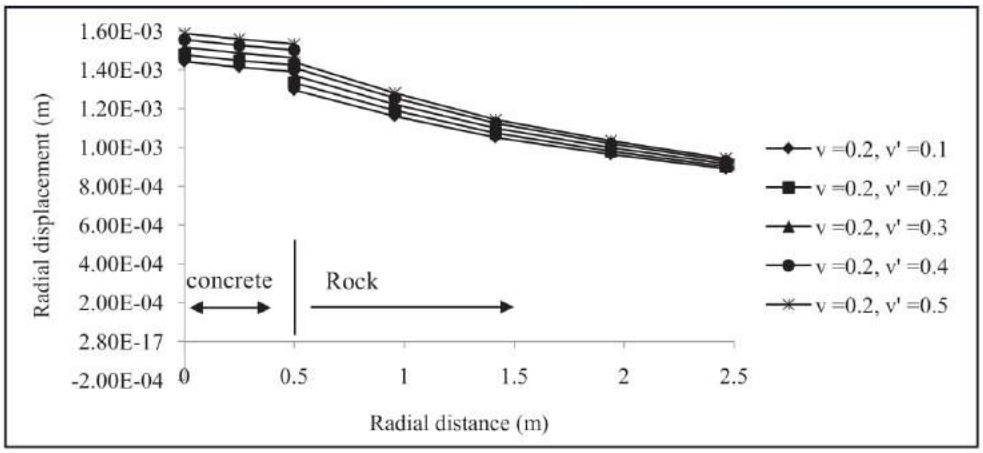

Fig. 24: Radial displacement variation along side wall for different ν' values

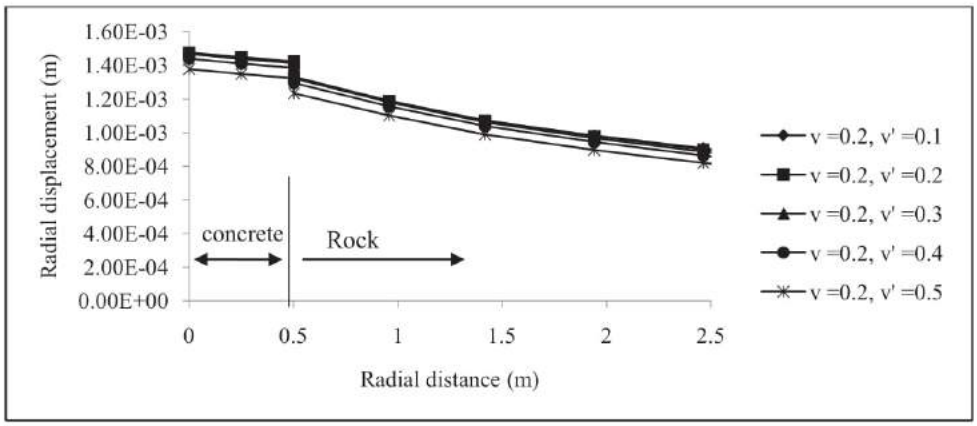

Fig. 25: Radial displacement variation along crown for different ν' values

Figures 24 and 25 show the radial displacement variation along sidewall and crown with radial distance for different ν' values varies from 0.1 to 0.5. As the ν' value is increased, the maximum radial displacements in the concrete lining are observed to increase where as it is observed to decrease along crown.

6. CONCLUSIONS

The following conclusions are drawn from the present study:

In lined pressure tunnels, maximum hoop stresses are concentrated in the concrete lining, whereas in the rock mass, they suddenly decrease with the change in the material properties.

As E/E' increases, the hoop stresses in the concrete lining are observed to be increased in the plane of transverse isotropy (side wall) of rock mass. Whereas in a direction normal to the plane of transverse isotropy (crown) of rock mass, as the E/E' ratio is increased the hoop stress variation is observed to be more uniform in the concrete lining.

As the E/E' ratio is increased the shear stresses are observed to increase along the concrete rock interface. A non-uniform shear stress variation is observed along concrete rock interface.

As G/G' increases, hoop stresses in the concrete lining are observed to increase in both the directions parallel (side wall) and normal to the plane of transverse isotropy (crown) of rock mass. Similar variation is observed along side wall and crown. The effect of shear modulus (G/G') is observed to be insignificant in shear stress distribution along concrete-rock interface.

As the ν' value is increased, a marginal decrease in the hoop stresses and a marginal increase in the shear stress are observed in the concrete lining. The effect of ν' is observed to be insignificant in radial stress and shear stress distribution.

References

Amadei B., Savage, W.Z. and Swolfs, H.S. (1987). Gravitational Stresses in Anisotropic Rock Mass, Int. J. of Rock Mech. Min. Sci., and Geomech. Abstr. 24, pp. 5-14.

Amadei B. (1996). Importance of Anisotropy When estimating and Measuring Insitu Stresses in Rock, Int. J. of Rock Mech. Min. Sci., and Geomech. Abstr., Vol. 33, No.3 pp 293-325.

Barla G. (1974). Rock Anisotropy: Theory and Laboratory Testing. In Rock Mechanics (edited by Muller), Udine, Italy pp. 131-169.

Jaeger, C. (1972). Rock Mechanics and Rock Engineering, Cambridge, Cambridge University Press.

Kumar, P and Singh, B. (1988). Pressure on Lining due to Initial Stress Field by Finite/Infinite/Interface Element Method, Rock Mechanics and Rock Engineering, 21, pp.219-228.

Kumar. P and Singh, Bhawani (1990). Design of Reinforced Concrete Lining on Pressure Tunnels, Considering Thermal Effects and Jointed Rock mass, J. of Tunnelling and Underground Space Technology, Vol. 5, No.12, pp. 91-101.

NISA (2007). User's Manual for NISA/CIVIL, Version 14.0, by Cranes Software International Limited, Bangalore.

Singh, B., Jethwa, J.L., Dube, A.K., (1995). Modified Terzaghi's Rock Load Concept for Tunnels, J. Rock. Mech. Tunnelling Technology, Vol.1, No.1 pp. 13-24.

Singh, B., Goel, R.K., Jethwa, J.L. and Dube, A.K. (1997). Support Pressure Assessment in Arched Underground Openings Through Poor Rock Masses, J. of Engineering Geology, Vol. 48, pp. 59-81.

Siva Parvathi, I., S. Surya Rao and Praveen, T.V. (2005). Effect of Rock Mass Quality and Tunnel Size on Lined Pressure Tunnels Using Finite Element Method, Journal of Rock Mechanics and Tunnelling Technology, Vol. 11, No.1, pp. 35-48.

Siva Parvathi, I., Praveen, T.V. and Suresh Kumar, K. (2013). Effect of Spacing and Orientation of Joints in the Rock on Stress Variation in Lined Pressure Tunnels Using Finite Element Method, Journal of Rock Mechanics and Tunnelling Technology, Vol. 19, No.1, pp. 1-17.

Siva Parvathi, I. and Praveen, T.V. (2015). Influence of Support Pressure on Stress Variation in Cracked Concrete Lined Pressure Tunnels, Journal of Rock Mechanics and Tunnelling Technology, Vol. 21, No.1, pp 7-20.

Terzaghi, K. (1946). Rock Defects and Load on tunnel Supports, Introduction to Rock Tunnelling with Steel Support, R.V. Proctor and T.C. White, Commercial Shearing and Stamping co., Youngstava, Ohio, USA.